

## Recycling of Al-rich industrial sludge in refractory ceramic pressed bodies

M.J. Ribeiro<sup>a</sup>, D.U. Tulyaganov<sup>b</sup>, J.M. Ferreira<sup>b</sup>, J.A. Labrincha<sup>b,\*</sup>

<sup>a</sup>ESTG, Polytechnique Institute of Viana do Castelo, 4900 Viana do Castelo, Portugal

<sup>b</sup>Ceramics and Glass Engineering Department, UIMC, University of Aveiro, 3810–193 Aveiro, Portugal

Received 16 July 2001; received in revised form 31 July 2001; accepted 9 September 2001

### Abstract

Processing of mullite-based refractory ceramic bodies by unidirectional dry pressing, from different formulations that include Al-rich sludge, as single or main component is described. The sludge is produced from anodising or surface coating processes and is generated in the wastewater treatment unit of an industrial plant. After a detailed characterisation study, involving determinations of chemical, thermal and granulometric parameters, as-received, and previously dried (110 °C) or calcined (1400 °C) sludge was used alone or combined with common ceramic raw materials, such as diatomite, kaolin or ball clay. Green bodies were consolidated by dry pressing and fired at temperatures in the range 1400–1650 °C, and the mechanical, thermal and electrical properties of the fired products were evaluated. Promising refractory materials based on mullite, mullite + alumina, or alumina were obtained. © 2002 Elsevier Science Ltd and Techna S.r.l. All rights reserved.

**Keywords:** Recycling; Al-rich industrial sludge; Refractory materials

### 1. Introduction

Aluminium anodising and powder surface coating processes are commonly used techniques to protect metallic bodies from corrosion effects and to achieve some aesthetic effects, such as colouring. These processes are highly water consuming, not only in each consecutive chemical batch but also to properly wash the pieces in between [1]. As a direct consequence, a huge amount of wastewater is generated and proper treatments are required to satisfy environmental criteria of the final generated effluent able to be sent out of the factory. Efficient solids removal and pH control of the suspension are the main required costly and time consuming operations [2,3]. Another consequence of these processes is the formation of high amounts of sludge, mostly constituted by colloidal aluminium hydroxide, sodium or calcium (generated from neutralising solutions) and aluminium (used as flocculating agent) sulphates, and water (up to 85 wt.%) [2,3].

Despite the potential high degree of metal mobility in aqueous solutions, this sludge has been often classified as

non-hazardous [4]. However, the high daily-producing amounts and the difficulties in reducing their volume, by suitable filter-pressing methods, require high transportation costs for disposal (22–30 US\$/ton). In EU countries, about 100 000 metric tonnes per year are currently generated [5] and no interesting applications were implemented up to now.

On the other hand, predictable high alumina contents of such calcined residues and their compositional constancy along the time makes them very attractive for recycling processes, such as trying to recover aluminium-based compounds, processing of alumina-based materials [6], or attempting to incorporate them in other products. In this last field, several materials have been investigated as inertization matrixes, such as concrete, glass and ceramics [7–9]. Some other possible applications for the raw Al-rich sludge have been attempted such as a glue for paper production [10], or as a sulphate-containing flocculation agent in wastewater purification processes [1].

This work aims to develop mullite or alumina-based ceramic refractories, shaped by unidirectional pressing of dried powder mixtures made of Al-rich sludge and common natural raw materials, such as kaolin, ball-clay and diatomite. These products should present high thermal inertness, electrical insulating properties, and strong mechanical strength. A detailed description about the

\* Corresponding author. Tel.: +351-2343-70250; fax: +351-2344-25300.

E-mail address: jal@cv.ua.pt (J.A. Labrincha).

processing and evaluation of the ultimate materials properties is given.

## 2. Experimental

### 2.1. Raw materials and batch formulations

The main component used to formulate several ceramic compositions was an Al-rich sludge generated in the wastewater treatment unit of an anodising or surface coating industrial plant (Extrusal, S.A., Aveiro) and used: (1) as-received and strongly humid (water content of about 85 wt.%), and (2) previously dried (at 110 °C for 24 h) or calcined (at 1400 °C for 2 h). The dried sludge is mostly constituted by aluminium hydroxide. Aluminium, calcium and sodium sulphates are also present as minor constituents. Its complete chemical and mineralogical characterisation is given elsewhere [4,5]. Calcination at 1400 °C decomposes all soluble salts and organic additives, and prevents the ulterior occurrence of possible deleterious phenomena or technological processing difficulties like high shrinkage levels, surfacial segregation, the formation of efflorescences or coloured spots, and mechanical deterioration. XRD analysis reveals the single presence of  $\alpha$ -Al<sub>2</sub>O<sub>3</sub> [5].

Other common Portuguese natural raw materials were used: (1) ball-clay (BM-8, Barracão); (2) kaolin (Mibal-B, Barqueiros); and (3) a previously calcined (at 600 °C, for 2 h) diatomite (Anglo-Portuguese Society of Diatomite, Óbidos). Their average chemical compositions were obtained by XRF and EDS and are given in Table 1.

XRD analysis revealed that the mineralogical constituents were: (1) kaolinite, quartz and traces of illite (ball-clay); (2) kaolinite, quartz, and small amounts of micaceous and feldspathic minerals (kaolin); (3) and basically amorphous silica (diatomite) [11].

The starting batch formulations are shown in Table 2, and the corresponding main oxide compositions estimated from the data given in Table 1 are also presented in Table 2. The use of as-received sludge was partially attempted in C3 formulation, while dried and calcined (at 1400 °C) sets were used in C1 and C2 compositions, respectively.

### 2.2. Preparation and characterization techniques

Starting aqueous suspensions having a solids load of 30–35 wt.% were deagglomerated and mixed by wet ball milling for 15 h, poured into plaster moulds to partially remove the water and then dried at 110 °C during about 24 h. The dried cakes were reduced to powders by deagglomeration in rapid porcelain jar mills for 15 min. Green bodies of different shapes and dimensions, rectangular (62×20 mm) and circular ( $\phi$ =25 mm) and about 3 mm thick were consolidated by uniaxial pressing at about 32 MPa. Bodies were then fired at different maximum temperatures, depending on the composition, namely, at 1400 and 1450 °C (C1); and at 1450, 1550, and 1650 °C (C2 and C3). Firing cycles correspond to heating and cooling rates of 5 °C/min and 1 h soaking at maximum temperature.

Particle size distributions of the as-received and dispersed sludge and of the several mixtures were measured by X-ray dispersion analysis (SediGraph 5100 V3.2—

Table 1  
Chemical compositions of raw materials determined by XRF and EDS (Al-sludge and diatomite)<sup>a</sup>

Raw material	SiO <sub>2</sub>	TiO <sub>2</sub>	Al <sub>2</sub> O <sub>3</sub>	Fe <sub>2</sub> O <sub>3</sub>	Cr <sub>2</sub> O <sub>3</sub>	CaO	MgO	SO <sub>3</sub>	K <sub>2</sub> O	Na <sub>2</sub> O	LOI
Al-sludge <sup>b</sup>	4.54	—	87.16	0.72	0.36	1.37	—	0.79	—	5.06	—
Kaolin Mibal-B <sup>c</sup>	47.00	0.20	37.10	1.10	—	0.10	0.15	—	2.00	0.20	12.15
Ball-clay	53.32	0.80	28.71	2.27	—	0.23	0.11	—	1.85	0.09	11.88
Diatomite <sup>d</sup>	92.30	—	1.40	1.80	—	1.80	—	—	2.70	—	—

<sup>a</sup> LOI, loss of ignition at 1000 °C.

<sup>b</sup> Calcined at 1400 °C for 2 h.

<sup>c</sup> As given by the supplier.

<sup>d</sup> Calcined at 600 °C for 2 h.

Table 2  
Tested batch formulations (wt.%) and corresponding chemical compositions adjusted and simplified to the Al<sub>2</sub>O<sub>3</sub>–SiO<sub>2</sub>–CaO ternary system

Composition	Al-sludge	Kaolin Mibal-B	Ball clay	Diatomite	Al <sub>2</sub> O <sub>3</sub>	SiO <sub>2</sub>	CaO
C1	79.5 <sup>a</sup>	—	—	21.5	63.5	29.5	8.2
C2	42 <sup>b</sup>	15	15	28	49.6	44.0	6.5
C3	100 <sup>c</sup>	—	—	—	86.5	4.5	9.1

<sup>a</sup> Dried sludge (110 °C for 24 h).

<sup>b</sup> Calcined sludge (1400 °C for 2 h).

<sup>c</sup> Mixture (50:50 wt.%) of wet (as-received) and calcined sludge.

Micromeritics). Apparent densities of fired bodies were determined by the Archimedes method (Hg immersion), while the real densities were measured by H<sub>2</sub>O pycnometry on grinded (<45 µm) sintered samples. Water absorption values were determined from the weight differences between the as-fired and water saturated samples (immersed for 2 h in boiling water) samples [12]. These values are related with the volume fraction of open pores (apparent porosity). Linear shrinkage values upon drying and firing were evaluated from the variation of the main dimension (length) of the parallelepipedic samples. The flexural strength (Lloyd Instruments LR 30K) of the sintered samples was the measured mechanical parameter. Dilatometric analysis (Netzsch 402 EP) was used to characterize the thermal expansion behaviour of dried and fired samples. Mineralogical characterization of the raw materials and determination of main crystalline phases formed during firing was done by XRD (Rigaku S4100) of fired bodies was also conducted on previously etched samples (5v/v HF solution for 2–5 min). Finally, electrical resistivity of Pt-electroded sintered samples was evaluated by impedance spectroscopy (HP 4284A, between 20 and 10 [6] Hz) as a function of temperature (600–1100 °C).

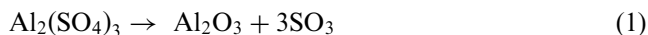
### 3. Results and discussion

#### 3.1. Sludge characterization

DTA/TGA curves of the wet (as-received) sludge are shown in Fig. 1. Removal of high amounts of free water or moisture is clearly denoted by the strong endothermic peak that occurs up to about 200 °C, corresponding to a weight loss of nearly 80%. A previous drying operation held at 110 °C for 24 h strongly reduces this phenomenon, as denoted by the lower weight changes on TGA curve. The gel-like consistency of the as-received sludge and the presence of significant amounts of hydroxides, are probably the main reasons for the

continuous weight loss observed for the dried sample up to about 500 °C.

DTA curve shows another endothermic inflection between 770 and 860 °C that might corresponds to the decomposition of aluminium sulphate:



Slight changes on TGA curves probably mean minor presence of this soluble salt.

Both TGA and DTA curves denote further decomposition reactions at temperatures higher than 1200 °C, probably due to the presence of different sulphates (Na and/or Ca), derived from the neutralizing batches of the anodising suspension. Therefore, a calcination step at 1400 °C was adopted to remove the soluble salts from the sludge and avoid unwanted problems related with differential migration or the formation of efflorescences.

Particle size analysis of the sludge (Fig. 2) confirms its fine character, being all particles inferior to 1 µm and the average size around 0.4 µm. This fineness might enhance mixing problems with other components and requires wet preparation processes that start from slurries.

Thermal expansion behaviour of the dry sludge is given in Fig. 3. A strong shrinkage (about 6%) is observed up to near 500 °C, certainly related with significant amount of released water (≈33.5 wt.%). This

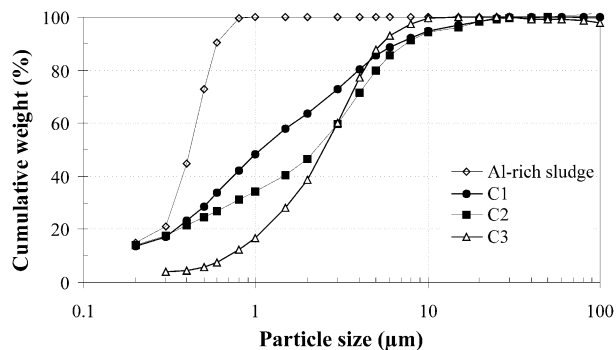


Fig. 2. Particle size distributions of different compositions and of the as-received dispersed sludge.

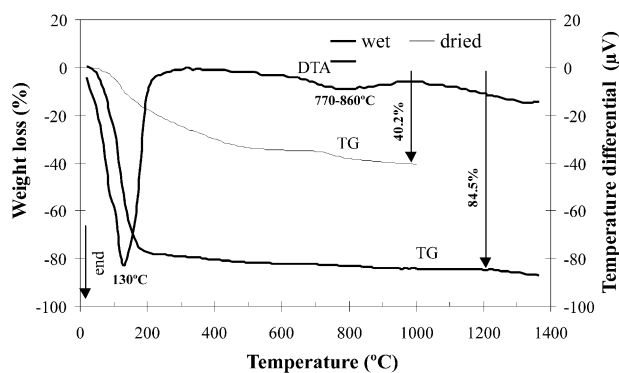


Fig. 1. TGA/DTA curves of wet and previously dried (at 110 °C) sludge.

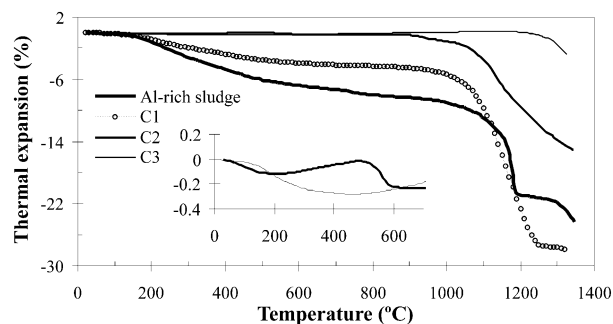


Fig. 3. Dilatometric curves of dried bodies made of several compositions and of pure sludge. Inserted picture gives a detailed view of the expansion behaviour of samples C2 and C3 up to about 600 °C.

observation confirms the need of a careful control of the heating process of pure or sludge-rich samples, to avoid deformation or failure risks. At about 1100 °C the abrupt collapse corresponds to starting of the sintering process. However, densification process seems to be stopped between 1200 and 1300 °C, probably due to gases release derived from decomposition of calcium sulphate. According to Mackenzie [13]  $\alpha \rightarrow \beta$  anhydrite transformation occurs at about 1225 °C before its decomposition into CaO and SO<sub>3</sub>. Above 1300 °C, densification process seems to restart.

### 3.2. Influence of composition and sintering temperature on the proprieties of ceramic bodies

Although the overall compositions of formulations C1, C2 and C3 are very complex, as shown in Table 1, the simplification attempt to represent them in the ternary equilibrium phase diagram of the main components SiO<sub>2</sub>–Al<sub>2</sub>O<sub>3</sub>–CaO [14] was made. Following this approach, similar oxides were grouped and converted

into the main representative oxide of each family (e.g. alkaline and earth-alkaline oxides were accounted as CaO, TiO<sub>2</sub> as SiO<sub>2</sub>, etc.). The simplified compositions are given in Table 2 and their locations in the phase diagram are shown in Fig. 4. Formulation C1 is closer to the mullite phase, and silica or alumina enrichment was tried with compositions C2 and C3, respectively. C2 belongs to the alumina-mullite-anorthite triangle and is located in the field of primary mullite (2Al<sub>2</sub>O<sub>3</sub>·SiO<sub>2</sub>) crystallization. C3 formulation is close to a pure alumina material and is located in corundum field. Its refractoriness is expectably higher. Final stable phases expected for C1 and C2 fired compositions are respectively mullite + alumina, and mullite + silica. XRD patterns (Fig. 5) partially confirm these predictions, except for C2 formulation where mullite is the single crystalline phase detected. In this case, silica might be dissolved in the glassy phase. C3 composition shows  $\beta$ -alumina (NaAl<sub>11</sub>O<sub>17</sub>) in addition to the predicted corundum, and in agreement with some previous results [5,7]. A combination of sodium in this phase should not affect the

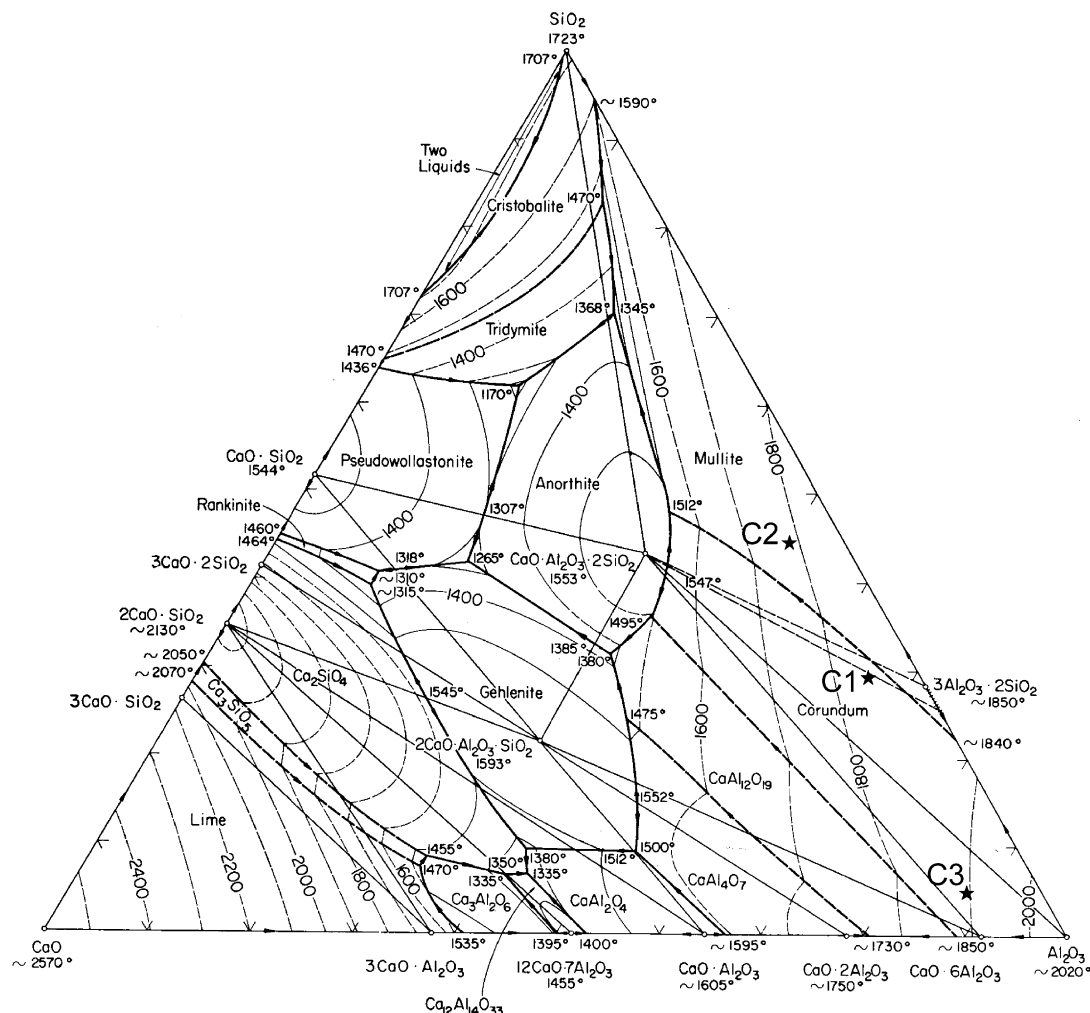


Fig. 4. Al<sub>2</sub>O<sub>3</sub>-SiO<sub>2</sub>-CaO equilibrium phase diagram showing the location of simplified C1, C2 and C3 compositions.

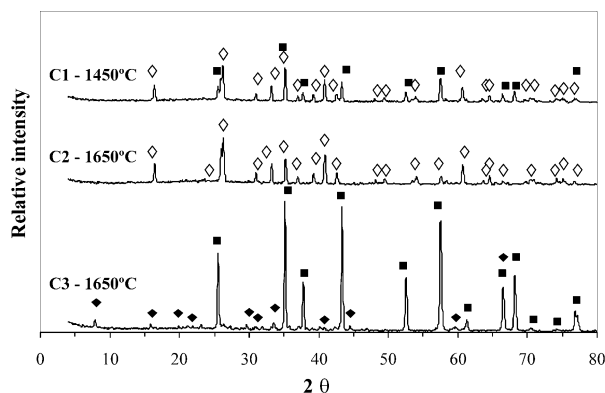
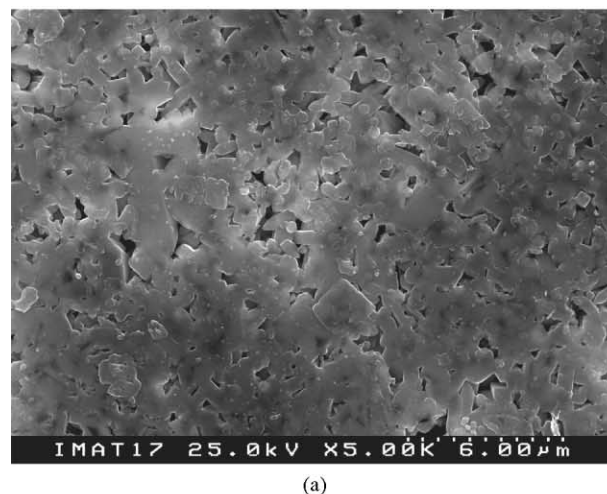


Fig. 5. XRD patterns of powdered samples of C1, C2 and C3 compositions fired at corresponding maximum temperatures ( $\diamond$ - mullite;  $\blacksquare$ ,  $\alpha$ -alumina;  $\bullet$ ,  $\text{NaAl}_{11}\text{O}_{17}$ ).

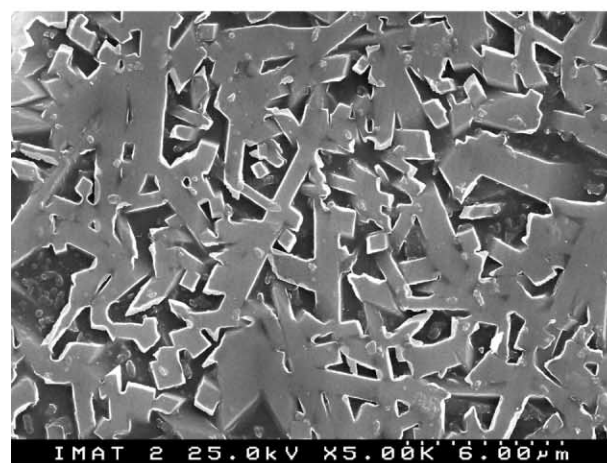
refractoriness of the material, since  $\beta$ -alumina is a well-known refractory inert material commonly used also as ionic conductor [15].

As predicted, C1 formulation is the highest reactive, and water absorption levels of only 1% were obtained for samples sintered at 1450 °C. In this material, the use of fine reactive dried sludge particles might favour earlier maturation processes. Fig. 6a shows a representative view of its microstructure, which confirms the presence of prismatic mullite grains involved by the glassy phase fulfilling the main portion of the inter-crystalline pores. On the contrary, the sintering of C2 and C3 compositions should be done at 1650 °C to get similar densification levels (Table 3). Real density values of C3 samples are clearly higher than the other formulations, due to the dominant presence of alumina (density of 3.98) [16]. Fig. 7 shows the microstructural evolution of C2 material with sintering temperature. Needle-like mullite small tertiary crystals are visible at 1450 °C and the amount of pores is still high. A more abundant glassy phase was formed at 1550 °C, enabling the growth of the mullite needles and fulfilling practically all the inter-crystalline pores. Only the larger inter-agglomerate pores are still visible. Finally, at 1650 °C large well-developed tabular crystals have been formed and all the pores seem to be covered by the glassy-phase (Fig. 6b).

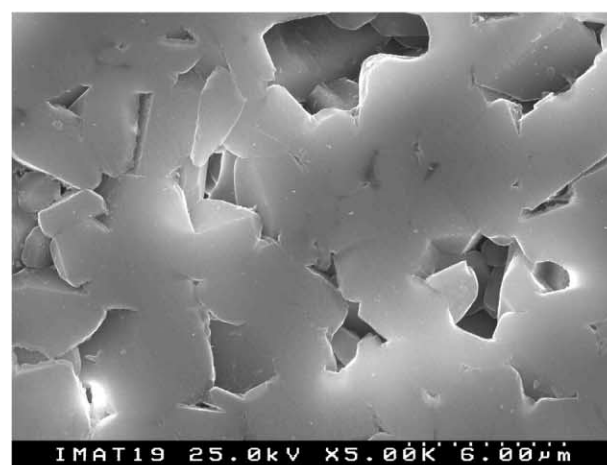
Mechanical and thermal expansion values, in addition to densification levels of tested samples, are summarized in Table 3 as a function of the sintering temperature. It can be seen that for all the compositions, density and bending strength values increase with increasing sintering temperatures. The highest value of bending strength ( $\approx 259$  MPa) was obtained for the composition C3 when fired at 1650 °C. This was expected from its higher alumina content and the less amount of glassy phase formed (Fig. 6c). Densified pure alumina bodies show flexural strength values higher than 310 MPa and their Moh's hardness is around 9 [16]. C2 samples are



(a)



(b)



(c)

Fig. 6. Typical microstructures of (a) C1, (b) C2, and (c) C3 samples fired at 1450 (the first one) and 1650 °C.

mechanically weak (only 58 MPa at 1650 °C), as predicted from the absence of alumina crystals in the ceramic matrix. In accordance to XRD results, single mullite crystals are observed surrounded by the glassy phase (Fig. 6b). This behaviour is also related with

Table 3  
Relevant characteristics of sintered bodies

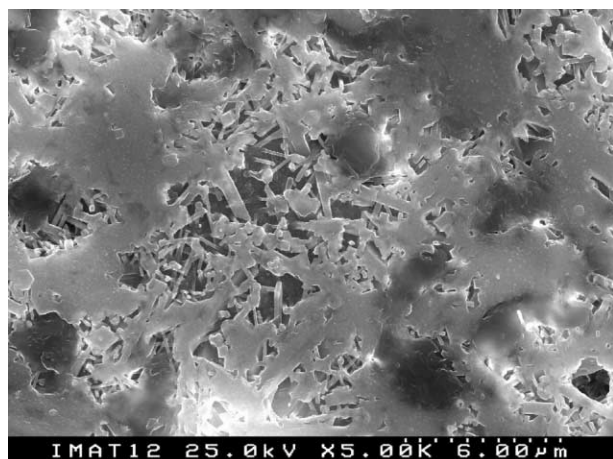
Composition	Sintering temperature (°C)	Bending strength (MPa)	Water absorption (%)	Apparent density (g/cm <sup>3</sup> )	Real density (g/cm <sup>3</sup> ) <sup>a</sup>	Densification (%)	Thermal expansion coefficient (20–°C) $\mu\text{m/m (}^{\circ}\text{C}^{-1}\text{)}$
C1	1400	47	2.87	2.65	–	88.9	–
	1450	86	0.06	2.80	2.98	94.0	6.702
	1450	35	39.72	2.13	–	76.6	5.25
C2	1550	38	7.51	2.23	–	80.2	5.67
	1650	58	0.69	2.50	2.78	89.9	5.62
	1450	56	22.9	1.95	–	54.0	–
C3	1550	159	7.54	2.70	–	74.8	–
	1650	259	0.08	3.29	3.61	91.1	8.41

<sup>a</sup> Determined by H<sub>2</sub>O pycnometry, as suggested by Sugiyama et al. [18].

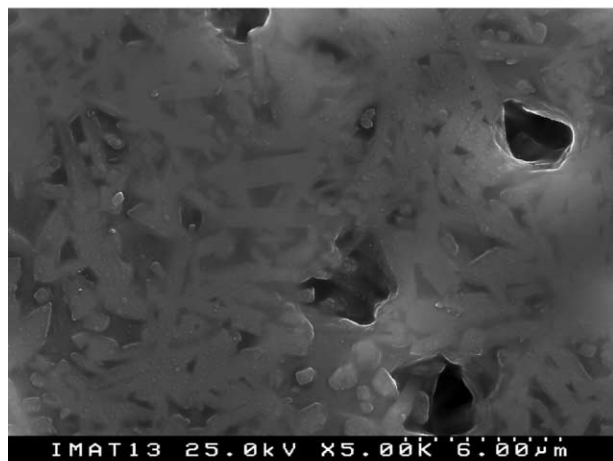
relatively lower densification levels, which are in accordance with higher water absorption values.

Thermal expansion behaviour of dried samples is shown in Fig. 3. The curve of C1 formulation is similar

to that of the pure dried sludge, in respect to the higher shrinkage values during the first heating stages (up to 1000 °C) and also in the occurrence of the mentioned non-densification step above 1200 °C. Overall shrinkage levels are also similar. We should keep in mind that this formulation contains dried sludge that will decompose upon firing. Densification process of C2 samples is delayed and less pronounced than that of C1 formulation, and only small shrinkage values can be observed up to 1200 °C, certainly due to the use of previously calcined sludge. These features are in accordance with lower final densification levels, already mentioned. Finally, the sintering process of C3 samples starts even at higher temperatures, despite the use of wet sludge. In comparison with C2 composition, slightly higher shrinkage is noticed at low temperatures (up to about 700 °C—see Fig. 3). However, the inertness character of the calcined sludge and the absence of clay-based components (that also decompose) or diatomite in the formulation C3 increase its refractoriness. We should also remind that after drying, the weight ratio between calcined and non-calcined sludge becomes about 50:25. The as-received wet sludge loses about 50% of its initial weight upon drying at 110 °C (Fig. 1). Shrinkage evolution above 1400 °C (Fig. 8) is in accordance with expansive tendencies now discussed.



(a)



(b)

Fig. 7. Microstructural evolution (SEM) of C2 samples as a function of the sintering temperature. (a) 1450 °C; (b) 1550 °C (the view of the sample sintered at 1650 °C is shown in Fig. 6).

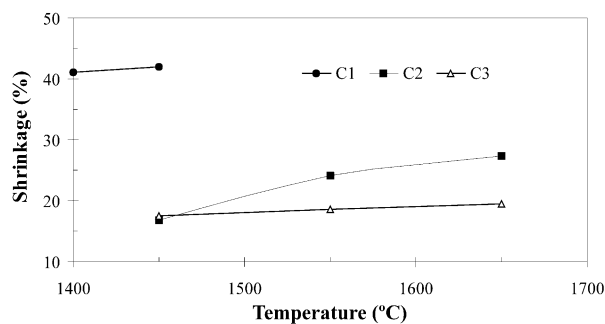


Fig. 8. Shrinkage evolution of all tested samples as a function of the sintering temperature.

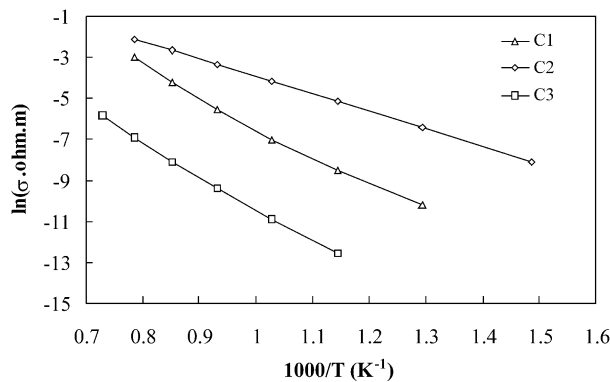


Fig. 9. Arrhenius plots of the electrical conductivity of all tested fired formulations, measured by impedance spectroscopy.

Similar dilatometric tests were conducted with sintered samples. Their average thermal expansion coefficients (Table 3) are comprised in the range between the average values of mullite ( $3.8 \times 10^{-6} \text{ K}^{-1}$ ) and alumina ( $8.0 \times 10^{-6} \text{ K}^{-1}$ ) [16,17]. Amongst all the compositions, C2 samples present the lowest values (about  $5.2\text{--}5.7 \times 10^{-6} \text{ K}^{-1}$ ), in accordance with SEM and XRD analyses that show the presence of single mullite crystals embedded in a silica-rich vitreous phase (low expansive, as well). On the contrary, C3 formulation is more expansive, being the values (about  $8.4 \times 10^{-6} \text{ K}^{-1}$ ) very similar to those of a pure alumina. C1 sintered material is made of alumina and mullite crystals (Fig. 6a) and its thermal behaviour traduces combined effects of both phases.

Electrical conductivity of samples was also measured as a function of the temperature (Fig. 9). All compositions show interesting insulating properties, being the C3 the highest resistive, as expected from its high alumina content. Resistivity values ( $\rho$ ) are comparable to those of a commercially-grade alumina. For example, current samples show  $\rho = 1.02 \times 10^5 \text{ } \Omega \text{ cm}$  at  $1000^\circ\text{C}$ , against  $5.0 \times 10^5 \text{ } \Omega \text{ cm}$  of a 94%-pure commercial material [17]. Lower values exhibited by the current samples are probably related with formation of incipient amounts of  $\beta$ -alumina and/or the presence of impurities. As observed for other characteristics, C2 formulation is the highest conductive ( $\rho = 8.94 \times 10^2 \text{ } \Omega \text{ cm}$  at  $1000^\circ\text{C}$ ) and C1 samples show intermediate values ( $\rho = 2.04 \times 10^3 \text{ } \Omega \text{ cm}$  at  $1000^\circ\text{C}$ ).

#### 4. Conclusions

The use of Al-rich sludge from anodising processes as the main component in the formulation of pressed bodies seems to be an interesting recycling destination for this abundant industrial waste. Its use (as-received and previously dried or calcined), as a single raw material or combined with common ceramic components, gives good controlled final compositions based on alumina,

mullite or mixtures of both phases after sintering at  $1450\text{--}1650^\circ\text{C}$ . The design of interesting technological properties, such as high electrical and mechanical resistance, refractoriness, etc., was found to be easily achievable by controlling the initial batch formulation and/or the sintering schedule. Its adaptability for several shaping techniques is now under progress.

#### Acknowledgements

Financial support from FCT (Portuguese Science Foundation) is greatly appreciated.

#### References

- [1] P. Pajunen, Chemical Recovery for Aluminum Finishers, Workshop on Cleaner Production in the Metal Finishing Industry, Taipei, Taiwan, April, 1999.
- [2] E. González, J.L. Asenjo, A. Baena, J. Dufour, A. La Iglesia, A. Hernández, N. Cornejo, E. Ruiz-Ayúcar, E. García, N. Ayayla, F. García-carcedo, F. Delmas, J.R. Mayarí, Application of anodising muds in several industrial fields, in: I. Gaballah, J. Hager, R. Solozabal (Eds.), Proceedings of the Rewas'99: Global Symposium on Recycling, Waste Treatment and Clean Technology, Vol. 1, San Sebastián, Spain, 1999, pp. 481–490.
- [3] J. Dufour, M.V. González, A. La Iglesia, Optimization model for the recovery of residual effluents of anodising industry, in: I. Gaballah, J. Hager, R. Solozabal (Eds.), Proceedings of the Rewas'99: Global Symposium on Recycling, Waste Treatment and Clean Technology, Vol. 1, San Sebastián, Spain, 1999, pp. 597–606.
- [4] A.M. Seabra, D.A. Pereira, C.M. Bóia, J.A. Labrincha, Pre-treatment needs for the recycling of Al-rich anodising sludge as a ceramic raw material, in: C.S. Gomes (Ed.), Proceedings of 1st Latin American Clay Conference, Vol. 2, Portuguese Clay Society, Funchal, Portugal, 2000, pp. 176–181.
- [5] D.A. Pereira, D.M. Couto, J.A. Labrincha, Incorporation of aluminum-rich residues in refractory bricks, CFI—Ceramic Forum International 77 (2000) 21–25.
- [6] D.A. Pereira, C.M. Bóia, J.A. Labrincha, Portuguese Patent No. 102573, 5 March 2001.
- [7] D.A. Tulyaganov, S.M. Olhero, M.J. Ribeiro, J.M. Ferreira, J.A. Labrincha, Mullite-alumina refractory ceramics obtained from mixtures of natural common materials and recycled Al-rich anodising sludge. J. Am. Ceram. Soc. (submitted for publication).
- [8] D.A. Pereira, J.B. Aguiar, F.P. Castro, M.F. Almeida, J.A. Labrincha, Mechanical behavior of Portland cement mortars with incorporation of Al-rich salt slags, Cement and Concrete Research 30 (2000) 1131–1138.
- [9] J.-H. Park, K.-H. Kim, J.-M. Cho, S.-K.M. Lim, Fabrication of  $\beta$ - and  $\beta'$ - $\text{Al}_2\text{O}_3$  tubes by pressureless powder packing forming and salt infiltration, J. Mater. Sci. 30 (1998) 5695–5702.
- [10] R.J. Brook (Ed.), Concise Encyclopedia of Advanced Ceramic Materials, Pergamon Press, New York, 1991.
- [11] P.V. Vasconcelos, J.A. Labrincha, J.M. Ferreira, Processing of diatomite from colloidal suspensions. Slip casting, Brit. Cer. Trans. 97 (1998) 24–28.
- [12] F. Andreola, C. Leonelli, M. Romagnoli, P. Miselli, Techniques used to determine porosity, Am. Ceram. Soc. Bull. July (2000) 49–52.

- [13] R.C. Mackenzie, Differential Thermal Analysis, Vol. 2, Academic Press, London, 1972.
- [14] Y. Takamiya, Y. Endo, S. Hosokawa (Eds.), Refractories Handbook, The Technical Association of Refractories, Japan, 1998.
- [15] D.C. Hitchcock, L.C. De Jonghe, Time-dependent degradation in sodium-beta alumina solid electrolytes, *J. Electrochem. Soc.* 133 (1986) 355–357.
- [16] Perry's Chemical Engineers Handbook, International 7th Edition, McGraw-Hill, 1997.
- [17] W.H. Gitzen (Ed.), Alumina as a Ceramic Material, The American Ceramic Society, OH, 1970.
- [18] N. Sugiyama, R. Harada, H. Ishida, Effect of alumina addition on the feldspathic porcelain bodies, *J. Ceram. Soc. Japan Int. Edition* 105 (1997) 134–139.